DALTON
FULL PAPER

Conformational control by halogen substitution and by crystallisation: a study of the molecular structures of $CH(SiMe_2H)_3$ and $CH(SiMe_2Br)_3$ by gas-phase electron diffraction, and *ab initio* molecular orbital calculations †

Carole A. Morrison,*[a] David W. H. Rankin,[a] Heather E. Robertson,[a] Colin Eaborn,[b] Adam Farook,[b] Peter B. Hitchcock[b] and J. David Smith*[b]

[a] *Department of Chemistry, University of Edinburgh, West Mains Road, Edinburgh, UK EH9 3JJ. E-mail: C.Morrison@ed.ac.uk*
[b] *School of Chemistry, Physics and Environmental Science, University of Sussex, Brighton, UK BN1 9QJ. E-mail: J.D.Smith@sussex.ac.uk*

Received 13th June 2000, Accepted 11th October 2000
First published as an Advance Article on the web 7th November 2000

The molecular structures of $CH(SiMe_2H)_3$ and $CH(SiMe_2Br)_3$ have been determined by gas-phase electron diffraction, *ab initio* calculations, and, for $CH(SiMe_2Br)_3$, X-ray diffraction. In each case, 11 distinct conformations, with energies lying within a range of 8.5 kJ mol^{-1} for $CH(SiMe_2H)_3$ and 26 kJ mol^{-1} for $CH(SiMe_2Br)_3$, were calculated and thus many conformers for both compounds are likely to exist in the gas phase. The structures are compared with those of related alkylsilanes to assess the changes in molecular geometry resulting from crowding at the carbon centre.

Introduction

The compounds described in this work, $CH(SiMe_2H)_3$ **1** and $CH(SiMe_2Br)_3$ **2**, are precursors for a remarkable series of organometallic compounds of the general type $MC(SiMe_2X)_3$ (X = OMe, NMe_2, PPh_2 or CH_2PPh_2, M = alkali metal or, for X = NMe_2, M = MgI), in which the organosilyl ligand is bound to the metal through both the central carbanionic site and the lone pairs of the group X. These compounds adopt a range of molecular or chain structures. For example, $LiC(SiMe_2CH_2PPh)_3$ **3**[1] and $MgIC(SiMe_2NMe_2)_3$ **4**[2] are monomeric with quite strong (**3**) or no (**4**) normal M···C bonds, $[LiC(SiMe_2OMe)_3]_2$ **5** is dimeric,[3] whereas $[LiC(SiMe_2NMe_2)_3]_\infty$ **6**[4] or $[KC(SiMe_2NMe_2)_3]_\infty$[5] are polymeric.

The range of different structures found in the solid state can be attributed in part to constraints in the metal co-ordination sphere, *e.g.* from size, valency and electronegativity, but in compounds containing very crowded ligands intra- as well as inter-ligand interactions can be important. For example, it has been suggested[5] that different intra-ligand Me···Me interactions may be important in accounting for the fact that **5** is oligomeric and **6** polymeric. It is thus of considerable interest to compare gas phase and solid state structures in order to determine more precisely the origin of the observed conformational effects and to distinguish those that are inherent within the ligand, from 'crystal packing forces' that are intermolecular.

The complexity of the intramolecular conformational effects is well illustrated by our previous gas-phase study of the compound $SiH_3C(SiMe_2H)_3$;[6] the vapour of which was surprisingly found to comprise a total of eleven structurally distinct conformers lying at points on the potential energy surface within a range of only *ca.* 3 kJ mol^{-1}. In compounds of the type $ZA(XY_3)_3$[7] or $A(XY_3)_4$,[6] 1,3-interactions between atoms or groups Y cause the XY_3 groups to twist away from perfectly staggered conformations, usually by 15–20°. All three or four branches must twist in the same sense. For $SiH_3C(SiMe_2H)_3$, therefore, to within a close approximation only three different values of the branch H_3Si–C–Si–H torsional angles were observed, *ca.* 160° (labelled type 'a'), 40° (type 'b') and −80° (type 'c'). The conformers are shown in Fig. 1. Three, labelled 'aaa', 'bbb' and 'ccc', have C_3 symmetry and eight, arising from all other possible combinations of the three different branch types, have C_1 symmetry. Whilst it is possible that mirror images of these branch dihedrals exist (*i.e.* −a, −b and −c) it is unlikely that combinations of these branch types with those found would give rise to additional minima. The differences between the values of the dihedral angles are of the order of 120°, giving rise

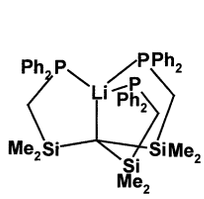

3

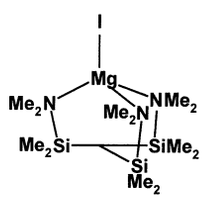

4

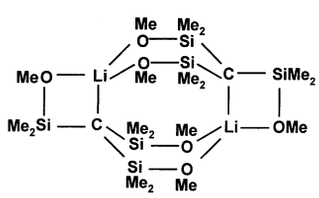

5

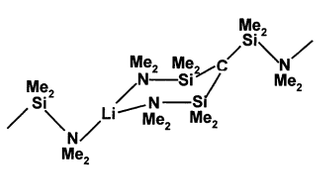

6

† Electronic supplementary information (ESI) available: gas phase electron diffraction (GED) results and rotatable pdb files for conformers. See http://www.rsc.org/suppdata/dt/b0/b004733n/

 DOI: 10.1039/b004733n

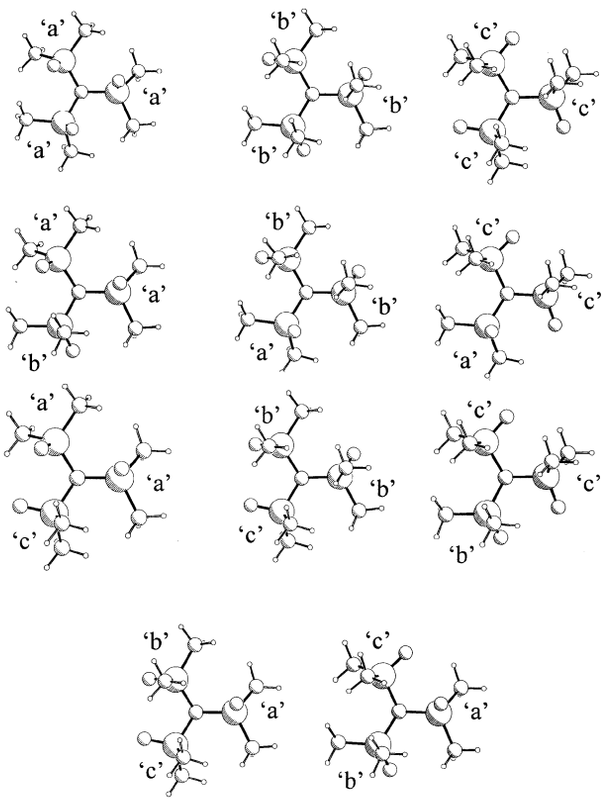

Fig. 1 Molecular structures of the eleven conformers of $CH(SiMe_2X)_3$ (X = H **1** or Br **2**). The hydrogen atom attached to the central carbon [denoted H(2) in the text] is not shown. Torsional angles H(2)–C(1)–Si–H are denoted 'a' *ca.* 160°, 'b' *ca.* 40° and 'c' *ca.* −80°.

to branches that are closely interlocked. Introducing a branch of opposite sign would reduce this angular separation, leading to increased steric crowding in the molecule.

In order to relate the data on $SiH_3C(SiMe_2H)_3$ to those on compounds of the type $MC(SiMe_2X)_3$ we chose to study the precursors **1** and **2** in some detail and found that the conformational effects were of considerable complexity. Here we present an account of the gas-phase structures and compare the data for **1** with those for related compounds. We determined the crystal structure of **2** in 1997[8] but withheld publication until we had the full electron diffraction data. Meanwhile, an independent account of the solid state structure of **2** has appeared.[9] Although our study gave bond lengths and angles with lower e.s.d.s we have not included the detailed results here.

Results

Ab initio molecular orbital calculations

A search of the potential energy surfaces of $CH(SiMe_2H)_3$ **1** and $CH(SiMe_2Br)_3$ **2** showed eleven different local minima for each compound, corresponding to those found for $SiH_3C(SiMe_2H)_3$. The minima for the hydride were found to lie within a range of *ca.* 8.5 kJ mol^{-1} on the potential energy surface (6-31G*/MP2), and indicated that nine of the eleven conformers would exist in significant proportions in the gas phase at the temperature of the GED experiment, and so should be modelled in the GED refinement. In contrast, the minima located for the bromide extended over a range of 26 kJ mol^{-1} (6-31G*/HF). Geometry optimisations at the computationally demanding 6-31G*/MP2 level were therefore only undertaken for the three lowest conformers of the bromo derivative. Partial geometries, obtained from the highest level calculations only, are given in Tables 1 and 2. [A full set of Brookhaven (pdb) coordinate files is available as ESI †] The absolute

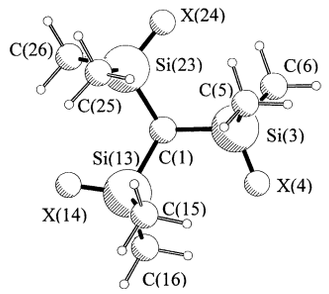

Fig. 2 Atom numbering scheme adopted for $CH(SiMe_2X)_3$ (X = H **1** or Br **2**). The hydrogen atom H(2) attached to the central carbon is not shown.

energies obtained in the 6-31G*/HF and 6-31G*/MP2 sets of calculations are listed in Table 3.

Gas-phase electron diffraction (GED)

Conformer weightings. The relative weightings of the conformers found for $CH(SiMe_2H)_3$ and $CH(SiMe_2Br)_3$ were derived by a consideration of the Boltzmann distribution of population states relative to the lowest energy conformer 'ccc' (see Table 3) and including the effects of multiplicity. In order to predict the energies of the minima at the temperatures of the GED data collection a thermal energy correction (calculated at 6-31G*/HF level, scale factor 0.9135‡) was applied to the absolute energies obtained at the 6-31G*/MP2 level. Changes in entropy (corrections also derived at 6-31G*/HF, scaled 0.9135‡) were found to be appreciable, and so relative abundances were derived from ΔG, not ΔH, values. On this basis, nine of the eleven conformers for $CH(SiMe_2H)_3$ and three for $CH(SiMe_2Br)_3$ were found to exist in sufficient quantity in the gas phase to be modelled in the GED refinements.

GED models. Full details of the mathematical models used to describe the nine conformers of $CH(SiMe_2H)_3$ and the three conformers of $CH(SiMe_2Br)_3$ predicted *ab initio* to exist in significant proportions in the gas phase can be found in the ESI,† and Tables 4 and 5. The atom numbering scheme is shown in Fig. 2.

GED refinements. *(a) $CH(SiMe_2H)_3$ **1**.* On the basis of the *ab initio* calculations detailed above, nine different conformers were modelled in the GED data collected for $CH(SiMe_2H)_3$, with the relative weightings fixed at computed values, given in the final column of Table 3.

The presence of large numbers of similar interatomic distances and of many distances of low multiplicity involving hydrogen (which is a poor scatter of electrons) prevented a complete structure determination for $CH(SiMe_2H)_3$ by use of expeimental data only, even with local symmetry approximations incorporated into the model. In such cases it is our practice to use the SARACEN method[11] which incorporates information obtained theoretically, and hence allows all parameters to be refined. The essential feature of this method is that data calculated *ab initio* are introduced into the refinement as additional observations (or restraints), the weight of any observation being assigned according to the level of convergence achieved in a series of graded *ab initio* calculations. By employing the SARACEN method in the present work it has been possible to refine the values of all structural parameters and all significant amplitudes of vibration. The final refinement is then the best fit to all available information, both experimental and

‡ Raw frequencies calculated at the Hartree–Fock level are known to contain systematic errors due to the neglect of electron correlation, resulting in overestimates of about 10–12%. It is therefore usual practice to scale zero-point energies and thermal energy corrections at the HF/6-31G* level by a scale factor of 0.9135.[10]

Table 1 Partial geometries of the eleven conformers of $CH(SiMe_2H)_3$ **1**[a] calculated *ab initio* at 6-31G*/MP2 (r_e/Å, ∠/°). Branch types 'a', 'b' and 'c' denote branch torsional angles H–C(1)–Si–H of *ca.* 160, 40 and −80°, respectively

	'aaa'	'bbb'	'ccc'	'aab'	'aac'	'bba'	'bbc'	'cca'	'ccb'	'abc'	'acb'
Bond distances											
*r*C(1)–H(2)	1.102	1.104	1.103	1.102	1.102	1.104	1.104	1.103	1.103	1.103	1.103
*r*C(1)–Si(3)	1.893	1.890	1.888	1.890	1.894	1.891	1.887	1.888	1.888	1.894	1.892
*r*C(1)–Si(13)	—	—	—	1.893	1.887	1.892	1.892	1.890	1.888	1.888	1.891
*r*C(1)–Si(23)	—	—	—	1.892	1.893	1.891	1.891	1.893	1.892	1.894	1.888
*r*Si(3)–H(4)	1.496	1.496	1.498	1.496	1.496	1.496	1.496	1.496	1.495	1.497	1.497
*r*Si(3)–C(5)	1.889	1.889	1.886	1.889	1.886	1.888	1.888	1.887	1.890	1.889	1.889
*r*Si(3)–C(6)	1.888	1.888	1.887	1.888	1.889	1.888	1.889	1.891	1.887	1.887	1.886
*r*Si(13)–H(14)	—	—	—	1.496	1.496	1.496	1.495	1.498	1.498	1.497	1.496
*r*Si(13)–C(15)	—	—	—	1.889	1.888	1.889	1.888	1.888	1.888	1.891	1.887
*r*Si(13)–C(16)	—	—	—	1.888	1.891	1.888	1.888	1.887	1.887	1.889	1.887
*r*Si(23)–H(24)	—	—	—	1.495	1.497	1.497	1.497	1.496	1.497	1.495	1.496
*r*Si(23)–C(25)	—	—	—	1.887	1.886	1.889	1.887	1.887	1.888	1.891	1.889
*r*Si(23)–C(26)	—	—	—	1.888	1.887	1.889	1.889	1.886	1.886	1.889	1.888
Bond angles											
∠H(2)–C(1)–Si(3)	107.1	104.3	105.1	105.9	106.6	105.5	104.5	105.8	104.8	105.4	105.6
∠H(2)–C(1)–Si(13)	—	—	—	106.6	106.4	104.8	104.5	105.9	105.1	105.9	105.7
∠H(2)–C(1)–Si(23)	—	—	—	106.4	106.6	105.7	104.9	105.7	104.9	105.5	105.3
∠Si(3)–C(1)–Si(13)	111.7	114.2	113.4	114.5	114.2	113.1	114.2	114.9	116.8	114.8	110.8
∠Si(3)–C(1)–Si(23)	—	—	—	111.6	108.1	114.1	116.4	112.2	111.5	109.4	112.7
∠Si(13)–C(1)–Si(23)	—	—	—	111.2	114.4	112.6	110.9	111.6	112.5	114.9	115.7
∠C(1)–Si(3)–H(4)	108.0	108.0	109.3	108.8	107.7	108.1	107.9	108.5	107.4	108.3	108.1
∠C(1)–Si(3)–C(5)	114.6	112.9	109.9	112.7	109.7	112.4	113.0	110.7	112.9	112.8	113.0
∠C(1)–Si(3)–C(6)	110.6	111.7	112.4	111.0	115.2	108.1	112.3	113.1	112.3	111.0	110.5
∠H(4)–Si(3)–C(5)	107.3	107.7	107.9	108.1	109.0	108.3	107.7	109.1	107.1	107.0	108.3
∠H(4)–Si(3)–C(6)	109.6	107.2	107.5	109.3	107.1	107.0	106.7	108.3	107.9	107.2	109.2
∠C(5)–Si(3)–C(6)	106.6	109.0	109.7	106.9	108.1	107.8	108.9	106.9	109.1	110.2	107.6
∠C(1)–Si(13)–H(14)	—	—	—	108.2	108.7	107.8	107.5	108.9	108.6	108.7	108.7
∠C(1)–Si(13)–C(15)	—	—	—	115.1	110.9	112.8	112.2	112.5	113.1	113.3	110.9
∠C(1)–Si(13)–C(16)	—	—	—	110.0	113.6	111.9	112.3	110.9	110.9	111.5	113.0
∠H(14)–Si(13)–C(15)	—	—	—	106.9	109.4	108.0	107.9	107.0	107.0	108.4	107.2
∠H(14)–Si(13)–C(16)	—	—	—	108.8	108.0	107.2	107.6	107.0	107.1	109.2	106.6
∠C(15)–Si(13)–C(16)	—	—	—	107.6	106.1	108.9	109.2	110.3	109.8	105.6	110.1
∠C(1)–Si(23)–H(24)	—	—	—	108.5	108.4	108.5	108.3	109.6	109.0	107.4	107.8
∠C(1)–Si(23)–C(25)	—	—	—	111.2	111.7	113.0	111.0	111.9	112.3	113.9	112.6
∠C(1)–Si(23)–C(26)	—	—	—	112.6	111.7	111.4	113.1	110.3	110.1	111.7	112.5
∠H(24)–Si(23)–C(25)	—	—	—	108.8	107.1	108.3	107.4	107.2	107.5	107.2	106.7
∠H(24)–Si(23)–C(26)	—	—	—	106.9	106.8	109.2	107.0	107.7	108.2	108.6	108.1
∠C(25)–Si(23)–C(26)	—	—	—	108.8	111.0	106.4	109.7	110.2	109.6	107.8	108.9
Torsional angles											
τH(2)–C(1)–Si(3)–H(4)	157.0	45.7	−81.9	163.3	152.9	46.2	47.5	167.7	46.2	−82.4	162.4
τH(2)–C(1)–Si(13)–H(14)	—	—	—	147.3	163.0	48.5	44.6	−83.2	−82.1	163.8	−83.4
τH(2)–C(1)–Si(23)–H(24)	—	—	—	50.0	−79.1	159.1	−83.7	−79.6	−83.2	45.9	48.7

[a] Conformers (in bold) included in the GED refinement.

theoretical, and represents the most probable structure, avoiding subjective preference for one particular type of data. The values of all additional observations used in the refinement can be found in Table 4, together with their respective uncertainties.

The results from the SARACEN refinement, based on GED data supplemented with *ab initio*-based restraints, are given in Table 4, together with the computed values.§ In general geometric parameters refined to values in good agreement with those calculated *ab initio*. Most notably the freely refining (*i.e.* unrestrained) parameters, which define the key features on the radial distribution curve [Fig. 3(a)], refined to values within acceptable ranges of calculated values. The average C–H distance (p_1) makes an unusually large contribution to the radial distribution curve and refined to 1.105(4) Å, compared with the *ab initio* value of 1.095 Å. The average Si–C distance (p_3, the second peak in the radial distribution curve) refined to 1.879(1) Å, compared with the average calculated value of 1.889 Å. The Si–C–H (methyl) angle (p_7), which in conjunction with p_1 and p_3 defines the position of the third peak on the radial distribution curve [labelled *r*H(Me)···Si], refined to 110.7(5)°. It thus falls near the middle of the range of values calculated for this angle (110.0–112.0°).

The branch angle C(1)–Si–C (p_8), which along with p_3 defines the positions of the C···C distances under the fourth peak, refined to 113.5(5)°, compared with the calculated range of angles 108.1–115.2°. The H(2)–C(1)–Si and average Si(branch)–C(1)–Si(branch) angles, p_6 and p_{10}, along with the Si–C distances, primarily define the location of the Si···Si distances under the fourth peak. Both angles refined to values within about two standard deviations of the calculated values.

The remaining parameters did not refine to realistic values when unrestrained, because they refer either to subtle geometry differences between correlated bond distances or angles (*i.e.* parameters 2, 4, 12 and 13) or to parameters involving hydrogen (parameters 5, 9, 10 and 14–38). These parameters were assigned *ab initio*-based restraints to aid their refinement. All restrained parameters returned values in the least-squares

§ For large, floppy molecules, such as those described here, it is not realistic to expect to obtain reliable r_a structures based on harmonic rectilinear (parallel and perpendicular) vibrational corrections. In particular, the perpendicular corrections are very poorly calculated, and introduce errors greater than those they are meant to solve. The structures presented in this paper are therefore of type r_a.

Table 2 Partial geometries of the significant conformers of $CH(SiMe_2Br)_3$ **2**[a] calculated *ab initio* (r_e/Å, ∠/°). Branch types 'a', 'b' and 'c' denote branch torsional angles H–C(1)–Si–Br of *ca.* 160, 40 and −80°, respectively

Basis set/ level of theory	'aaa' 6-31G*/HF	'bbb' 6-31G*/HF	'**ccc**' 6-31G*/MP2	'**aab**' 6-31G*/MP2	'aac' 6-31G*/HF	'**bba**' 6-31G*/MP2	'bbc' 6-31G*/HF	'cca' 6-31G*/HF	'ccb' 6-31G*/HF	'acb' 6-31G*/HF	'abc' 6-31G*/HF
Bond distances											
*r*C(1)–H(2)	1.098	1.092	1.104	1.105	1.097	1.103	1.092	1.095	1.093	1.094	1.094
*r*C(1)–Si(3)	1.907	1.907	1.896	1.894	1.915	1.895	1.902	1.916	1.915	1.899	1.912
*r*C(1)–Si(13)	—	—	—	1.889	1.904	1.888	1.914	1.906	1.901	1.905	1.905
*r*C(1)–Si(23)	—	—	—	1.894	1.907	1.889	1.907	1.908	1.911	1.917	1.908
*r*Si(3)–Br(4)	2.238	2.248	2.272	2.258	2.240	2.254	2.245	2.256	2.254	2.254	2.249
*r*Si(3)–C(5)	1.879	1.883	1.871	1.871	1.879	1.874	1.882	1.880	1.878	1.882	1.881
*r*Si(3)–C(6)	1.883	1.878	1.872	1.875	1.881	1.874	1.883	1.877	1.881	1.879	1.878
*r*Si(13)–Br(14)	—	—	—	2.248	2.243	2.253	2.242	2.256	2.259	2.245	2.249
*r*Si(13)–C(15)	—	—	—	1.873	1.881	1.874	1.880	1.881	1.880	1.880	1.878
*r*Si(13)–C(16)	—	—	—	1.876	1.882	1.873	1.881	1.878	1.881	1.882	1.883
*r*Si(23)–Br(24)	—	—	—	2.252	2.250	2.261	2.244	2.244	2.240	2.247	2.247
*r*Si(23)–C(25)	—	—	—	1.873	1.876	1.872	1.881	1.885	1.879	1.877	1.883
*r*Si(23)–C(26)	—	—	—	1.875	1.885	1.874	1.883	1.877	1.886	1.882	1.879
Bond angles											
∠H(2)–C(1)–Si(3)	101.8	104.4	104.7	104.5	102.1	104.7	104.2	103.1	103.3	103.3	103.0
∠H(2)–C(1)–Si(13)	—	—	—	104.8	102.6	105.4	104.1	103.8	103.5	103.8	104.3
∠H(2)–C(1)–Si(23)	—	—	—	103.6	102.8	104.6	103.5	103.0	103.7	103.8	103.0
∠C(1)–Si(3)–Br(4)	110.3	107.7	109.4	105.8	110.2	106.0	108.6	111.2	111.4	108.1	108.1
∠C(1)–Si(3)–C(5)	115.9	113.0	112.1	114.2	110.8	114.3	113.6	110.6	110.9	116.1	116.4
∠C(1)–Si(3)–C(6)	110.0	116.2	113.6	114.1	115.6	115.1	114.8	113.9	113.5	112.8	112.1
∠Br(4)–Si(3)–C(5)	106.4	106.7	103.0	107.3	108.7	106.5	107.3	102.4	103.6	105.1	104.6
∠Br(4)–Si(3)–C(6)	107.4	104.1	104.1	103.8	105.1	104.4	103.5	105.2	104.1	108.3	109.6
∠C(5)–Si(3)–C(6)	106.3	108.3	113.6	110.7	106.1	109.6	108.4	112.7	112.7	106.0	105.7
∠C(1)–Si(13)–Br(14)	—	—	—	107.1	109.5	107.0	107.6	110.6	110.4	111.0	107.9
∠C(1)–Si(13)–C(15)	—	—	—	116.6	111.8	112.9	112.9	111.9	112.5	113.8	114.0
∠C(1)–Si(13)–C(16)	—	—	—	111.4	116.0	114.8	115.7	114.5	114.0	111.3	115.0
∠Br(14)–Si(13)–C(15)	—	—	—	106.1	108.2	107.3	108.5	102.9	103.0	105.4	107.7
∠Br(14)–Si(13)–C(16)	—	—	—	108.5	104.9	104.4	103.7	104.5	104.8	103.5	103.4
∠C(15)–Si(13)–C(16)	—	—	—	106.8	105.9	109.8	107.9	111.5	111.2	111.1	108.1
∠C(1)–Si(23)–Br(24)	—	—	—	109.2	110.3	106.9	112.2	108.4	108.3	106.8	111.6
∠C(1)–Si(23)–C(25)	—	—	—	117.0	114.6	117.9	111.2	114.7	113.8	114.0	110.7
∠C(1)–Si(23)–C(26)	—	—	—	109.9	111.1	111.2	113.5	113.4	114.2	115.0	114.4
∠Br(24)–Si(23)–C(25)	—	—	—	105.3	107.1	104.8	103.7	104.8	109.0	108.4	102.6
∠Br(24)–Si(23)–C(26)	—	—	—	107.2	102.3	108.1	104.6	110.0	103.0	103.2	106.0
∠C(25)–Si(23)–C(26)	—	—	—	107.8	110.8	107.4	111.0	105.1	107.8	108.6	110.7
Torsional angles											
τH(2)–C(1)–Si(3)–Br(4)	155.9	43.2	−83.1	42.7	−153.0	38.3	43.3	−83.5	−86.7	161.3	160.1
τH(2)–C(1)–Si(13)–Br(14)	—	—	—	164.4	−162.0	48.6	35.6	−77.6	−77.7	−75.1	43.0
τH(2)–C(1)–Si(23)–Br(24)	—	—	—	150.2	71.9	157.1	−81.0	163.8	36.5	31.2	−77.4

[a] 'ccc', 'aab' and 'bba' (in bold) are the conformers included in the GED refinement.

Table 3 Absolute energies (calculated *ab initio*) and relative abundance of all conformers modelled in the electron diffraction analysis

Conformer[a]	Multiplicity	Energy (Hartrees) 6-31G*/HF	Energy (Hartrees) 6-31G*/MP2	Thermal energy correction (343/410 K) 6-31G*/HF (scaled 0.9135)	Absolute energy ($H^{343,410}$)	$T\Delta S$ (T = 343/410 K) 6-31G*/HF (scaled 0.9135) (Hartrees)	Free energy ($G = H^{343,410} - T\Delta S$)	Population[b] (based on free energy)
$CH(SiMe_2H)_3$								
'aaa'	1	−1144.708434	−1145.881112	0.285120	−1145.595992	0.079335	−1145.675327	~0.00
'bbb'	1	−1144.709619	−1145.882304	0.284859	−1145.597445	0.079456	−1145.676901	~0.00
'ccc'	1	−1144.712447	−1145.883894	0.284809	−1145.599084	0.081080	−1145.680164	0.13
'aab'	3	−1144.709618	−1145.882108	0.284970	−1145.597138	0.081276	−1145.678414	0.08
'aac'	3	−1144.709818	−1145.881918	0.284994	−1145.596924	0.081163	−1145.678087	0.06
'bba'	3	−1144.709215	−1145.881709	0.284947	−1145.596971	0.082077	−1145.679048	0.14
'bbc'	3	−1144.709942	−1145.882364	0.284878	−1145.597486	0.080656	−1145.678142	0.06
'cca'	3	−1144.711113	−1145.882756	0.284891	−1145.597865	0.081820	−1145.679685	0.24
'ccb'	3	−1144.710868	−1145.882892	0.284859	−1145.598033	0.080839	−1145.678872	0.11
'acb'	3	−1144.710413	−1145.882426	0.284905	−1145.597521	0.081157	−1145.678678	0.10
'abc'	3	−1144.709025	−1145.881464	0.284576	−1145.596888	0.081527	−1145.678415	0.08
$CH(SiMe_2Br)_3$								
'aaa'	1	−8852.847476	—	—	—	—	—	~0.00
'bbb'	1	−8852.848743	—	—	—	—	—	~0.00
'ccc'	1	−8852.856491	−8854.375376	0.280884	−8854.094492	0.122952	−8854.217444	0.76
'aab'	3	−8852.852067	−8854.369866	0.280636	−8854.089230	0.123683	−8854.212913	0.09
'aac'	3	−8852.848854	—	—	—	—	—	~0.00
'bba'	3	−8852.852503	−8854.370114	0.280637	−8854.089476	0.124026	−8854.213502	0.15
'bbc'	3	−8852.846044	—	—	—	—	—	~0.00
'cca'	3	−8852.851351	—	—	—	—	—	~0.00
'ccb'	3	−8852.848702	—	—	—	—	—	~0.00
'acb'	3	−8852.849887	—	—	—	—	—	~0.00
'abc'	3	−8852.849240	—	—	—	—	—	~0.00

[a] See text and Fig. 2 for structural definitions. [b] Calculated on the basis of a Boltzman distribution, relative to the lowest energy conformer 'ccc' [343 K for $CH(SiMe_2H)_3$, 410 K for $CH(SiMe_2Br)_3$]. Abundances were then normalised, allowing for multiplicities.

Table 4 Structural parameters for $CH(SiMe_2H)_3$ obtained by gas-phase electron diffraction and *ab initio* calculations (r/Å, ∠/°)

	Parameter[a]	GED (restrained results) (r_a)[b]	*Ab initio* (6-31G*/MP2) (r_e)[c]
Independent parameters			
p_1	rC–H (Me + central)	1.105(4)	av. 1.095
p_2	Δ rC–H (Me − central)	0.010(1)	0.010(1)
p_3	av. rSi–C (middle + branch)	1.879(1)	av. 1.889
p_4	Δ rSi–C (middle − branch)	0.003(1)	0.003(1)
p_5	rSi–H	1.496(2)	1.496(2)
p_6	∠H(2)–C(1)–Si (branch)	104.9(3)	av. 105.5
p_7	∠Si–C–H (Me)	110.7(5)	range 110.0–112.0
p_8	∠C(1)–Si–C (branch)	113.5(5)	range 108.1–115.2
p_9	∠C(1)–Si–H (branch)	109.0(8)	108.3(10)
p_{10}	∠H–Si–C	108.7(6)	107.8(10)
p_{11}	∠Si–C(1)–Si ('w' + 'm' + 'n')	113.5(7)	av. 112.1
p_{12}	Δ ∠Si–C(1)–Si ['w' − av. ('m' + 'n')]	3.3(5)	3.2(5)
p_{13}	Δ ∠Si–C(1)–Si ('m' − 'n')	1.3(5)	1.3(5)
p_{14}	'ccc' τH(2)–C(1)–Si–H	−81.2(17)	−81.9(20)
p_{15}	'cca' τH(2)–C(1)–Si(3)–H(4)	−79.2(18)	−79.6(20)
p_{16}	'cca' τH(2)–C(1)–Si(3)–H(14)	−83.0(18)	−83.2(20)
p_{17}	'cca' τH(2)–C(1)–Si(3)–H(24)	168.3(18)	167.7(20)
p_{18}	'ccb' τH(2)–C(1)–Si(3)–H(4)	−82.8(18)	−83.2(20)
p_{19}	'ccb' τH(2)–C(1)–Si(3)–H(14)	−81.9(18)	−82.1(20)
p_{20}	'ccb' τH(2)–C(1)–Si(3)–H(24)	47.0(18)	46.2(20)
p_{21}	'bba' τH(2)–C(1)–Si(3)–H(4)	46.4(18)	46.2(20)
p_{22}	'bba' τH(2)–C(1)–Si(13)–H(14)	48.8(18)	48.5(20)
p_{23}	'bba' τH(2)–C(1)–Si(23)–H(24)	159.2(18)	159.1(20)
p_{24}	'bbc' τH(2)–C(1)–Si(3)–H(4)	47.8(18)	47.5(20)
p_{25}	'bbc' τH(2)–C(1)–Si(13)–H(14)	44.8(18)	44.6(20)
p_{26}	'bbc' τH(2)–C(1)–Si(23)–H(24)	−83.5(18)	−83.7(20)
p_{27}	'aac' τH(2)–C(1)–Si(3)–H(4)	153.1(18)	152.9(20)
p_{28}	'aac' τH(2)–C(1)–Si(13)–H(14)	163.1(18)	163.0(20)
p_{29}	'aac' τH(2)–C(1)–Si(23)–H(24)	−78.8(18)	−79.1(20)
p_{30}	'aab' τH(2)–C(1)–Si(3)–H(4)	163.3(18)	163.3(20)
p_{31}	'aab' τH(2)–C(1)–Si(3)–H(14)	147.3(18)	147.3(20)
p_{32}	'aab' τH(2)–C(1)–Si(3)–H(24)	50.3(18)	50.0(20)
p_{33}	'acb' τH(2)–C(1)–Si(3)–H(4)	49.0(18)	48.7(20)
p_{34}	'acb' τH(2)–C(1)–Si(3)–H(14)	−83.3(18)	−83.4(20)
p_{35}	'acb' τH(2)–C(1)–Si(3)–H(24)	162.2(18)	162.4(20)
p_{36}	'abc' τH(2)–C(1)–Si(3)–H(4)	−82.1(18)	−82.4(20)
p_{37}	'abc' τH(2)–C(1)–Si(13)–H(14)	164.0(18)	163.8(20)
p_{38}	'abc' τH(2)–C(1)–Si(23)–H(24)	46.1(18)	45.9(20)
Dependent parameters			
	rSi–C (middle)	1.880(1)	av. 1.891
	rSi–C (branch)	1.878(1)	av. 1.888
	rC(1)–H(2)	1.110(4)	av. 1.10
	rC–H(Me)	1.100(4)	av. 1.09
	∠Si–C(1)–Si ('w')	115.7(7)	av. 114.0
	∠Si–C(1)–Si ('m')	113.1(8)	av. 112.0
	∠Si–C(1)–Si ('n')	111.8(8)	av. 110.0

[a] See ESI for model description. Note: 'middle' = rSi(3,13 or 23)–C(1) and 'branch' = rSi–C(Me) distances (see Fig. 2 for atom numbering scheme). Abbreviations used: r = bond distance, ∠ = angle, τ = dihedral angle, Me = methyl, av. = average, Δ = difference, 'a,b,c' = branch types, 'w,m,n' = wide, middle, narrow; see the ESI and Fig. 2 for details. [b] Estimated standard deviations (e.s.d.s) obtained in the least-squares refinement are given in parentheses. [c] Some *ab initio* data are quoted with values in parentheses. These are the uncertainties derived from the series of calculations that determine the weights given to the restraints. *Ab initio* values quoted as averages are derived from values calculated for each given parameter averaged over all the conformers.

analysis in agreement with their imposed restraints to within one esd.

In addition to all 38 geometric parameters, five amplitudes of vibration, corresponding to groups of similar distances under the four most prominent peaks on the radial distribution curve, were also refined. The groups chosen correspond to all C–H distances for the nine conformers under peak 1, the Si–C distances under peak 2, rH(Me)···Si (peak 3) and the Si···Si distances under peak 4. All amplitudes refined to reasonable values, in good agreement with those calculated *ab initio*.

The final R_G factor recorded for this nine-conformer refinement is 0.095, indicating that a satisfactory fit between model and experiment has been obtained. The final experimental and difference radial distribution curves and molecular scattering curves are shown in Figs. 3(a) and 1(a) of the ESI,† respectively. Selected tables are available in the ESI, comprising a full set of coordinates (Table 1), a listing of bond distances and amplitudes of vibration common to all nine conformers (Table 2), and the final correlation matrix (Table 3).

*(b) $CH(SiMe_2Br)_3$ **2**.* Obtaining a satisfactory fit to the experimental data for the bromo derivative proved to be harder than for the hydride. There are several reasons for this. First, the compound is more reactive chemically and so two attempts were required to obtain a satisfactory data set. Secondly, as the compound contains many heavy atoms that are strong scatterers of electrons the choice of starting geometry in the least-squares refinement procedure proved to be of paramount importance. Thirdly, on the basis of the *ab initio* calculations, the gaseous sample was expected to be a three-component mixture, comprising 76% of 'ccc', 9% of 'aab' and 15% of 'bba' (see

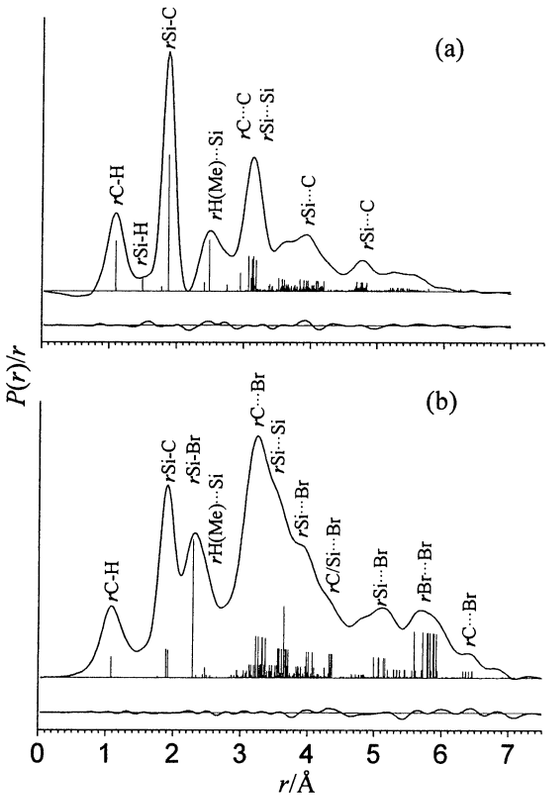

Fig. 3 Experimental and difference (experimental − theoretical) radial distribution curves for the multi-conformer analyses of (a) $CH(SiMe_2H)_3$ and (b) $CH(SiMe_2Br)_3$. Before Fourier inversion the data were multiplied by $s \cdot \exp(-0.002s^2)/(Z_{Si} - f_{Si})(Z_{C(or\ Br)} - f_{C(or\ Br)})$.

Table 3). However, all attempts to refine the three-conformer mixture fixed in these proportions resulted in an unsatisfactory fit to the experimental data ($R_G > 0.16$). It was found that a satisfactory fit could be obtained only by reducing the abundance of the 'ccc' conformer to about 33%, with the same weighting for conformers 'aab' and 'bba'. It is impossible to confirm the exact proportions of the gas phase mixture on the basis of electron diffraction data alone, as varying the proportions of the three-component mixture by up to 20% from equal weightings did not result in any appreciable deterioration in the fit. It is also impossible to rule out the possibility that other conformers may be present in the gaseous mixture. What is clear, however, is that the gas is not largely composed of just one conformer, as suggested by the *ab initio* calculations.

Once values for the abundances of the three conformers that gave reasonable agreement with experimental data had been obtained, the refinement proceeded smoothly to completion. As the bromo derivative contains three heavy atoms, fewer parameter restraints were required than for the hydride. The only parameters that required restraint were the H–C(1)–Si angle, p_6, the torsion angles involving hydrogen (p_{25-30}) and those parameters describing subtle differences between correlated distances (p_2, p_4, $p_{9,10}$, $p_{12,13}$, and $p_{15,16}$). The results from the refinement are given in Table 5, together with values derived computationally.

The key features on the radial distribution curve [Fig. 3(b)] were defined by freely refining parameters, which in general gave acceptable agreement with the calculated values. The first three peaks are attributed to *r*C–H, *r*C–Si (two distances) and *r*Si–Br, which all refined to values within 0.02 Å of the average calculated values. The low intensity distance at 2.47 Å, giving rise to the slight shoulder on the third peak, allowed the refinement of p_6, the Si–C–H (methyl) angle, to near exact agreement with the calculated value. The fourth peak (from 3–4.5 Å), comprising a peak and three shoulders, conceals a plethora of mostly *r*C/Si · · · Br distances. Their positions are largely dictated by the heavy-atom angles p_{8-21}, several of which refined to values 2–5° narrower than those calculated (see Table 5). The intense contributions from long-range Br · · · Br distances all fell under the peak at 5.5–6.0 Å, with the exception of *r*Br(13) · · · Br(23) in conformer 'aab', which at 3.69(12) Å (*cf.* 4.01 Å calculated) fell under the fourth peak. It is possible that some of the differences between experiment and theory can be attributed to a shrinkage effect in the experimental data, arising from the fact that vibrational averaging gives rise to long-range distances appearing to be shorter than the sum of their constituent bonding distances. Such an effect should be quite small, however, and to a certain extent the low symmetry model should make allowances for this. A more likely source of error is in the level of calculations performed, with a double-zeta quality basis set for bromine probably not adequate to give completely reliable geometries.

In addition to all 30 geometric parameters, ten amplitudes of vibration, corresponding to groups of similar distances under the six prominent peaks on the radial distribution curve, were also refined. With reference to Fig. 3(b) they were chosen as the C–H distances (peak 1), the Si–C distances (peak 2), *r*Si–Br (peak 3), *r*C · · · Br (*ca.* 3.25 Å), *r*Br · · · Si (3.6–3.7 Å), *r*Br · · · Si (4.0–4.1 Å) and *r*Br · · · Si (4.3–4.35 Å) (all peak 4), *r*Si · · · Br (5.0–5.2 Å, peak 5), *r*Br · · · C (5.3–5.45 Å, also peak 5) and finally *r*Br · · · Br (5.6–5.9 Å, peak 6).

The final R_G factor recorded for this three-conformer refinement is 0.097, indicating that a satisfactory fit between model and experiment has been obtained. The final radial distribution and molecular scattering curves (experimental and difference) are shown in Fig. 3(b) and Fig. 1(b) of the ESI, respectively. The remaining experimental information (a full set of coordinates, a listing of distances and amplitudes of vibration refined in the analysis, and the final correlation matrix) is deposited in the ESI in Tables 4–6, respectively.

Discussion

Molecular conformations

For all three compounds, $CH(SiMe_2H)_3$ **1**, $CH(SiMe_2Br)_3$ **2**, and $SiH_3C(SiMe_2H)_3$ **7**,[6] *ab initio* calculations predict the 'ccc' conformation, in which the three atoms of X (H or Br) are as far apart as possible, to be the most stable. The fact that this arrangement is the most stable both for compound **1** containing the $SiMe_2H$ and for compound **2** containing the $SiMe_2Br$ group indicates that crowding between methyl groups as well as between bromine atoms is important. Intramolecular Me · · · Me interactions are minimised in the 'ccc' arrangement since the six methyl groups are separated into two groups of three, whereas in the 'aaa' and 'bbb' arrangements all six methyl groups are crowded together.

The unsymmetrical configurations, which are shown by the calculations to have only slightly higher energies than the 'ccc' arrangement, are obtained by exchanging Me groups for X by rotation about Si–C bonds so that the Me groups are distributed over the surface of the molecule. For $SiH_3C(SiMe_2H)_3$ **7**, which is roughly spherical, the relative energies fall in a narrow range (*ca.* 3 kJ mol^{-1}) but for the less symmetrical, more oblate $CH(SiMe_2H)_3$ **1** a wider variety of methyl group environments is possible and the energy range spanned by the various conformers greater. Nevertheless it is still necessary to take account of nine of these in modelling the electron diffraction data.

Crowding is significantly increased by replacing Si–H by Si–Br bonds, so that in $CH(SiMe_2Br)_3$ the range of conformers spans an energy range of 26 kJ mol^{-1} and only three, *viz.* 'ccc', 'bba' and 'aab', are predicted *ab initio* to be present in appreciable quantities in the gaseous phase. This result cannot be explained simply in terms of minimising Br · · · Br interactions. The symmetrical conformer has the longest mean Br · · · Br distance and the 'bba' conformer the next longest, but several

Table 5 Structural parameters for $CH(SiMe_2Br)_3$ obtained by gas-phase electron diffraction and *ab initio* calculations (r/Å, ∠/°)

	Parameter[a]	GED (restrained results) (r_a)[b]	*Ab initio* (6-31G*/MP2) (r_e)[c]
Independent parameters			
p_1	rC–H (Me + central)	1.084(8)	av. 1.095
p_2	Δ rC–H (Me − central)	0.010(7)	0.010(5)
p_3	av. rSi–C (middle + branch)	1.898(2)	av. 1.879
p_4	Δ rSi–C (middle − branch)	0.024(6)	0.024(5)
p_5	rSi–Br	2.283(8)	av. 2.260
p_6	∠H(2)–C(1)–Si (branch)	104.6(7)	av. 104.6
p_7	∠Si–C–H (Me)	109.4(13)	av. 109.0
p_8	av. ∠C(1)–Si–C (branch) ('w' + 'm' + 'n')	109.1(9)	av. 114.2
p_9	Δ ∠C(1)–Si–C (branch) ['w' − av. ('m' + 'n')]	3.7(13)	5.0(10)
p_{10}	Δ ∠C(1)–Si–C ('m' − 'n')	2.8(14)	3.0(10)
p_{11}	∠C(1)–Si–Br ('w' + 'm' + 'n')	105.6(10)	av. 109.4
p_{12}	Δ ∠C(1)–Si–Br ['w' − av. ('m' + 'n')]	1.1(13)	2.8(10)
p_{13}	Δ ∠C(1)–Si–Br ('m' − 'n')	1.0(14)	1.0(10)
p_{14}	av. ∠Br–Si–C ('w' + 'm' + 'n')	102.5(13)	av. 105.5
p_{15}	Δ ∠Br–Si–C ['w' − av. ('m' + 'n')]	3.3(13)	3.0(10)
p_{16}	Δ ∠Br–Si–C ('m' − 'n')	1.5(14)	2.0(10)
p_{17}	'ccc' ∠Si–C–Si distortion1	1.1(7)	1.0(5)
p_{18}	'ccc' ∠Si–C–Si distortion2	−0.9(7)	−1.0(5)
p_{19}	∠Si–C–Si 'aa'	119(3)	115.2
p_{20}	∠Si–C–Si 'bb'	110(3)	112.2
p_{21}	∠Si–C–Si 'ba'	115.2(12)	av. 113.0
p_{22}	'ccc' τC(1)–Si(2)–Si–H (average)	−78(3)	−83.1
p_{23}	'ccc' Δ τC(1)–Si(2)–Si–H	5.0(7)	5.0(5)
p_{24}	'ccc' Δ τC(1)–Si(2)–Si–H	2.4(7)	2.5(5)
p_{25}	'aab' τH(2)–C(1)–Si(13)–H(4)	40(3)	40(2)
p_{26}	'aab' τH(2)–C(1)–Si(23)–H(14)	157(3)	160(2)
p_{27}	'aab' τH(2)–C(1)–Si(3)–H(24)	160(3)	160(2)
p_{28}	'bba' τH(2)–C(1)–Si(13)–H(4)	36(3)	38(2)
p_{29}	'bba' τH(2)–C(1)–Si(23)–H(14)	48(3)	49(2)
p_{30}	'bba' τH(2)–C(1)–Si(3)–H(24)	155(3)	157(2)
p_{31}	weight 'ccc'	0.3333	0.76
p_{32}	weight 'bba'	0.3333	0.15
Dependent parameters			
	rSi–C (middle)	1.914(5)	av. 1.893
	rSi–C (branch)	1.889(5)	av. 1.873
	rC(1)–H(2)	1.089(10)	av. 1.10
	rC–H(methyl)	1.079(7)	av. 1.09
	∠C–Si–Br ('w')	106.3(9)	av. 109.3
	∠C–Si–Br ('m')	105.7(14)	av. 107.0
	∠C–Si–Br ('n')	104.7(15)	av. 106.0
	∠Br–Si–C ('w')	104.7(18)	av. 107.5
	∠Br–Si–C ('m')	102.2(16)	av. 105.5
	∠Br–Si–C ('n')	100.6(13)	av. 103.5
	∠C(1)–Si–C ('w')	111.6(14)	av. 117.5
	∠C(1)–Si–C ('m')	109.2(10)	av. 114.0
	∠C(1)–Si–C ('n')	106.5(12)	av. 111.0
	'ccc' ∠Si(3)–C(1)–Si(13)	112.8(8)	113.8
	'ccc' ∠Si(13)–C(1)–Si(23)	114.6(9)	113.8
	'ccc' ∠Si(23)–C(1)–Si(3)	114.1(11)	113.8
	weight 'aab'	0.3333	0.09

[a] See ESI for model description. Note: 'middle' = rSi(3, 13 or 23)–C(1) and 'branch' = rSi–C(methyl) distances (see Fig. 2 for atom numbering scheme). Abbreviations used: r = bond distance, ∠ = angle, τ = dihedral angle, Me = methyl, av. = average, Δ = difference, 'a,b,c' = branch types, 'w,m,n' = wide, middle, narrow; see the ESI and Fig. 2 for details. [b] Estimated standard deviations (e.s.d.s) obtained in the least-squares refinement are given in parentheses. [c] Some *ab initio* data are quoted with values in parentheses. These are the uncertainties derived from the series of calculations that determine the weights given to the restraints. *Ab initio* values quoted as averages are derived from values calculated for each given parameter averaged over all the conformers.

other conformations have higher mean Br···Br distances than those of the 'aab' conformer (see Fig. 1). The presence of this conformer, with two upward pointing Br atoms, in the gas phase suggests that Me···Me interactions are of similar importance to Br···Br interactions in determining the overall conformational stability and is in accord with the fact that Me and Br have been assigned similar van der Waals radii.[12] It is not possible to deduce from the gas-phase data why the 'aab' conformer is found in the crystal.

The conformers of **2** are interconverting rapidly on the NMR timescale in toluene-d_8 at −90 °C.[9] The failure of the calculations on the bromo derivative to predict the correct relative populations of the different conformers is probably an artefact of the quality of the calculations, with a larger basis set than that of 6-31G* being required for bromine. Unfortunately calculations of this magnitude are not possible with our current computational resources.

Structure of $CH(SiMe_2Br)_3$ 2

Results from X-ray and electron diffraction and from *ab initio* calculations are given in Table 6. The Si–Br and C–Si distances obtained by electron diffraction appear to be longer than those from X-ray diffraction but experimental uncertainties are such

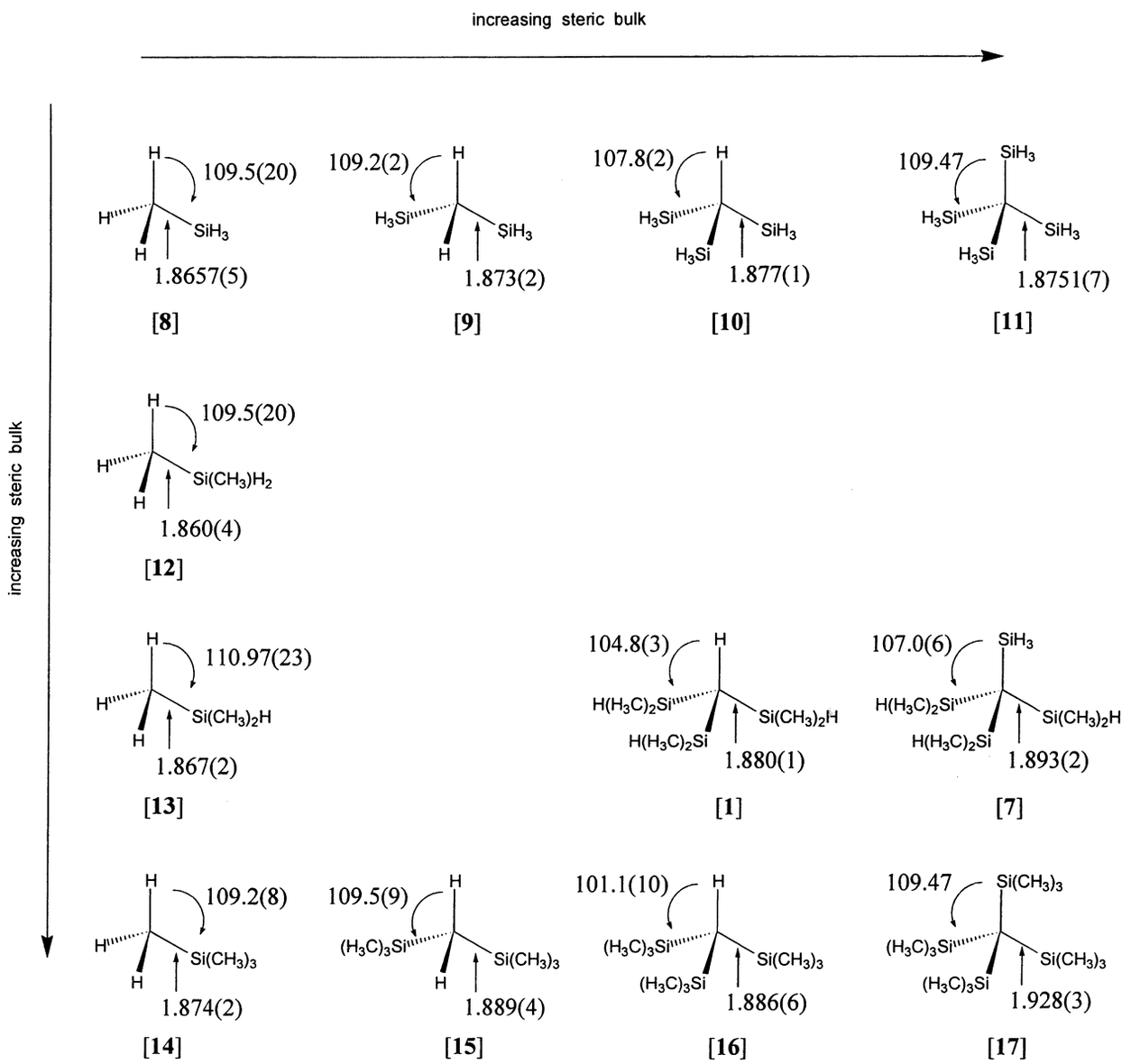

Fig. 4 Molecular structures of related crowded silanes determined by microwave spectroscopy or electron diffraction. References: [**8**]: R. W. Kilb and L. Pierce, *J. Chem. Phys.*, 1957, **27**, 108. [**9**]: A. Almenningen, H. M. Seip and R. Seip, *Acta Chem. Scand.*, 1970, **24**, 1697. [**10**]: H. Schmidbaur, J. Zech, D. W. H. Rankin and H. E. Robertson, *Chem. Ber.*, 1991, **124**, 1953. [**11**]: R. Hager, O. Steigelmann, G. Müller, H. Schmidbaur, H. E. Robertson and D. W. H. Rankin, *Angew. Chem., Int. Ed. Engl.*, 1990, **29**, 201. [**12**]: A. C. Bond and L. O. Brockway, *J. Am. Chem. Soc.*, 1954, **76**, 3312. [**13**]: L. Pierce and D. H. Petterson, *J. Chem. Phys.*, 1960, **33**, 907. [**1**]: This work. [**7**]: C. A. Morrison, D. W. H. Rankin, H. E. Robertson, P. D. Lickiss and P. C. Masangane, *J. Chem. Soc., Dalton Trans.*, 1999, 2293. [**14**]: B. Beagley, J. J. Monaghan and T. G. Hewitt, *J. Mol. Struct.*, 1971, **8**, 401. [**15**]: T. Fjeidberg, R. Seip, M. F. Lappert and A. J. Thorne, *J. Mol. Struct.*, 1983, **99**, 295. [**16**]: B. Beagley and R. G. Pritchard, *J. Mol. Struct.*, 1982, **84**, 129. [**17**]: B. Beagley, R. G. Pritchard and J. O. Titiloye, *J. Mol. Struct.*, 1988, **176**, 81. Note that all Si–C distances have been converted to r_a with the exception of [**12**], for which no mention of the structural type was reported in the literature.

Table 6 Comparison of electron diffraction and X-ray data for $CH(SiMe_2Br)_3$ **2**. Bond lengths/Å, angles/°. E.s.d.s of individual measurements in parentheses

	X-Ray[a]	GED	*ab initio* (6-31G*/MP2)
*r*Si–Br	2.251(3)–2.263(3)	2.283(8)	2.250
*r*C(1)–Si	1.883(5)–1.885(7)	1.914(5)	1.892
*r*Si–Me	1.846(9)–1.871(10)	1.889(5)	1.874
∠Si–C–Si	114.4(4)–115.9(4)	113.8(10)	113.8
∠C(1)–Si–Me	112.4(4)–115.6(4)	111.6(14)	114.2
∠C(1)–Si–Br	106.6(3)–108.3(3)	106.3(9)	107.4

[a] Ref. 9. More accurate data are found in ref. 8.

that it is not clear whether the differences in values from the two techniques are significant. No significant differences are apparent in the values of the bond angles derived by the various techniques. Few crystallographic data for bonds between bromine and four-coordinate silicon have appeared in the literature. The Si–Br bond length in **2** [2.257(2) Å] is longer than those in the bromosilanes $SiMe_nBr_{4-n}$ [2.175(1)–2.235(2) Å], $BrSiH_2CH_2CH_2SiH_2Br$ [2.2362(12) Å][13] and 1-bromo-3,5,7-trimethyl-1,3,5,7-tetrasilaadamantane (2.197 Å),[14] but a little shorter than those [2.284(5), 2.283(1) Å] in two sterically encumbered polysilanes.[15]

Molecular structures of crowded alkylsilanes

The molecular structures of a number of alkylsilanes **7**–**17** have been studied over the last 50 years by electron diffraction and microwave spectroscopy and some of the structural parameters obtained (all reduced to a common r_a structure) are shown in Fig. 4. In the least sterically crowded silane $MeSiH_3$ **8** the C–Si bond length is 1.8657(5) Å and the H–C–Si angle 109.5(20)°, the same as that in a perfect tetrahedron. Substitution of the three hydrogen atoms bound to silicon by more bulky methyl

Table 7 GED data analysis parameters

Compound	Camera distance/mm	Weighting functions /Å^{-1}					Correlation parameter	Scale factor, k [a]	Electron wavelength [b]/pm
		Δs	s_{min}	sw_1	sw_2	s_{max}			
$CH(SiMe_2H)_3$	257.03	0.2	3.0	4.0	13.0	15.2	0.4567	0.756(7)	0.06016
	97.75	0.4	12.0	12.8	30.5	35.6	0.1469	0.808(26)	0.06016
$CH(SiMe_2Br)_3$	257.08	0.2	2.0	4.0	9.6	10.0	0.3783	0.794(24)	0.06016
	97.85	0.4	9.6	10.0	26.0	28.4	−0.2802	1.67(13)	0.06016

[a] Figures in parentheses are the estimated standard deviations. [b] Determined by reference to the scattering patterns of benzene vapour.

groups (**12**→**14**) results in a barely significant change in the C–Si bond length and no significant change in the H–C–Si angle. The effect of substitution of the hydrogen atoms of the methyl group by more bulky SiH_3 groups, shown in the series **9**→**11**, likewise gives only a small change in the C–Si bond length. Crowding at the carbon centre is shown by a significant decrease in the H–C–Si angle to 107.8(2) in the trisilane $CH(SiH_3)_3$ **10** but the C–Si bond length is essentially unchanged in the tetrasilane **11**, in which the configuration at the central carbon is forced by symmetry to be exactly tetrahedral.

The data for $CH(SiMe_2H)_3$ **1** given in the present work, together with those for $SiH_3C(SiMe_2H)_3$ **7** reported previously,[6] make it possible to assess the effects of replacing the hydrogens of the methyl group in the $MeSiH_3$ skeleton with $SiMe_2H$ groups. The increase in C–Si from 1.867(2) Å in CH_3SiMe_2H **13** to 1.880(1) Å in $CH(SiMe_2H)_3$ **1** and 1.893(2) Å in $SiH_3C(SiMe_2H)_3$ **7** is significant. However, the crowding of the $SiMe_2H$ substituents is partly offset by contraction of the H–C–Si angle (which is a little greater than the tetrahedral value in **13**) to 104.8(3)° in **1** and partly by changes in the H–C–Si–H torsion angles from the values of 160, 40 and −80° imposed by near tetrahedral symmetry in $SiH_3(SiMe_2H)_3$. Similar trends are observed in the series from CH_3SiMe_3 **14** to $C(SiMe_3)_4$ **17**. There is considerable narrowing of the H–C–Si angle in the triorganosilyl derivative $CH(SiMe_3)_3$ and the C–Si bond, though longer than that in $SiMe_4$, is significantly shorter than the central bond in the very crowded $C(SiMe_3)_4$. Crowding is markedly increased as the hydrogen atoms attached to silicon in **1** and **7** are replaced by methyl groups, as shown by the lengthening of the Si–C bonds and, for the compounds **1** and **16**, a decrease in the H–C–Si angle. Changing the central H atom for the more bulky SiH_3 or $SiMe_3$ substituent has little effect on the Si–C bond length when the remaining branches are not bulky (**10**→**11**), but when they are the X–C–Si angle widens by more than 2° and the C–Si bond length increases by more than 0.01 Å to accommodate the bigger central group (**1**→**7**). If tetrahedral symmetry is enforced the C–Si bond lengthens by more than 0.04 Å to reduce molecular crowding (**16**→**17**).

Conclusion

The work described here on compounds **1** and **2** provides a nice example of the use of the SARACEN technique to facilitate the refinement of intractable structures based on electron diffraction data. It shows that with these complex sterically crowded molecules a number of conformations have similar absolute energies and therefore may be present in appreciable concentrations at quite low temperatures (350–400 K). Crowding between methyl groups as well as bromine atoms is important. The work also shows the limitations of information on crowding provided by X-ray diffraction alone; the conformation in the crystal is only one of those present in the gas. The range of structures found for the molecules **1** and **2** is reminiscent of the wide range of configurations of the $C(SiMe_2Ph)_3$ fragment observed in previous crystallographic studies.[16] Though it is not possible to explain these in detail, the conformational variety is not now surprising in view of the complexity shown by the simpler $CH(SiMe_2H)_3$ and $CH(SiMe_2Br)_3$ derivatives.

Experimental

Synthesis

The compounds **1** and **2** were made as described in the literature and spectroscopic data agreed with those previously reported.[17]

Ab initio molecular orbital calculations

Calculations were performed on a DEC Alpha APX 1000A workstation using the GAUSSIAN98 program,[18] with the larger calculations run on a DEC 8400 superscalar cluster equipped with 10 fast processors, 6 GB of memory and 150 GB disk (resource of the UK Computational Chemistry Facility).

Geometry optimisations

Extensive searches of the potential energy surfaces for $CH(SiMe_2H)_3$ and $CH(SiMe_2Br)_3$ were undertaken at the 3-21G*/HF level in order to locate all structurally stable conformers. In total eleven minima were found for both compounds, corresponding to three structures with C_3 symmetry and eight with C_1 (Fig. 1). Further geometry optimisations were then undertaken for all minima with the 6-31G* basis set at the HF level of theory, and for all energetically significant minima at the higher level 6-31G*/MP2.

Frequency calculations

Vibrational frequencies were calculated from analytic second derivatives at the 3-21G*/HF and 6-31G*/HF levels to confirm that all stationary points found were local minima on the potential energy surface. The force constants obtained from the 6-31G*/HF calculations were subsequently used to construct harmonic force fields using the ASYM40 program.[19] As no fully assigned vibrational spectra are available for these compounds to scale the force fields, a scaling factor of 0.9 was applied to all symmetry coordinates, as the neglect of electron correlation in a vibrational frequency calculation is known to overestimate vibrational frequencies by about 10%.[10] The scaled harmonic force fields were then used to provide estimates of amplitudes of vibration (u) for use in the GED refinements.

Gas-phase electron diffraction

Electron scattering intensities were recorded on Kodak Electron Image photographic plates using the Edinburgh gas-phase electron diffraction apparatus,[20] operating at *ca.* 40 kV. Five plates (three from the long camera distance and two from the short distance) were obtained for $C(SiMe_2H)_3H$ and four plates (two long and two short) for $CH(SiMe_2Br)_3$. Data from all plates were converted into digital format using a computer-controlled PDS microdensitometer employing a 200 micron pixel size at the Royal Greenwich Observatory, Cambridge.[21] The sample and nozzle temperatures were maintained at *ca.* 343 K and 390 K during the exposure periods for the hydride and bromide, respectively. Standard programs and scattering factors[22] were used for the data reduction.[23] Nozzle-to-plate distances, weighting functions used to set up the off-diagonal

weight matrices, correlation parameters, final scale factors and electron wavelengths for the measurements are given in Table 7.

Acknowledgements

We thank the EPSRC for financial support of the Edinburgh Electron Diffraction Service (grant GR/K44411), the Edinburgh *ab initio* facilities (grant GR/K04194) and research at Sussex (grant GR/L83585). We also thank the UK Computational Chemistry Facility (admin: Department of Chemistry, King's College London, Strand, London, UK WC2R 2LS) for the computing time on Columbus and the Malaysian Government for a scholarship to A. F.

References

1 A. G. Avent, D. Bonafoux, C. Eaborn, M. S. Hill, P. B. Hitchcock and J. D. Smith, *J. Chem Soc.*, *Dalton Trans.*, 2000, 2183.
2 C. Eaborn, A. Farook, P. B. Hitchcock and J. D. Smith, *Organometallics*, 1997, **16**, 503.
3 F. I. Aigbirhio, N. H. Buttrus, C. Eaborn, S. H. Gupta, P. B. Hitchcock, J. D. Smith and A. C. Sullivan, *J. Chem. Soc.*, *Dalton Trans.*, 1992, 1015.
4 A. Farook, C. Eaborn, P. B. Hitchcock and J. D. Smith, *Chem. Commun.*, 1996, 741.
5 S. S. Al-Juaid, C. Eaborn, S. El-Hamruni, A. Farook, P. B. Hitchcock, M. Hopman, J. D. Smith, W. Clegg, K. Izod and P. O'Shaughnessy, *J. Chem. Soc.*, *Dalton Trans.*, 1999, 3267.
6 C. A. Morrison, D. W. H. Rankin, H. E. Robertson, P. D. Lickiss and P. C. Masangane, *J. Chem. Soc.*, *Dalton Trans.*, 1999, 2293.
7 N. H. Buttrus, C. Eaborn, M. N. A. El-Kheli, P. B. Hitchcock, J. D. Smith, A. C. Sullivan and K. Tavakkoli, *J. Chem. Soc.*, *Dalton Trans.*, 1988, 381.
8 A. Farook, D. Phil. Thesis, University of Sussex, 1998.
9 D. M. Friesen, R McDonald and L. Rosenberg, *Can. J. Chem.*, 1999, **77**, 1931.
10 *Exploring Chemistry with Electronic Structure Methods*, ed. J. B. Foresman and Æ. Frish, Gaussian, Inc., Pittsburgh, PA, 2nd edn., 1996.
11 A. J. Blake, P. T. Brain, H. McNab, J. Miller, C. A. Morrison, S. Parsons, D. W. H. Rankin, H. E. Robertson and B. A. Smart, *J. Phys. Chem.*, 1996, **100**, 12280; P. T. Brain, C. A. Morrison, S. Parsons and D. W. H. Rankin, *J. Chem. Soc.*, *Dalton Trans.*, 1996, 4589.
12 A. Bondi, *J. Phys. Chem.*, 1964, 68, 441; L. Pauling, *The Nature of the Chemical Bond*, Cornell University Press, Ithaca, N.Y., 3rd edn., 1960, p. 261.
13 E. Lukevics, O. Pudova and R. Sturkovich, *Molecular Structure of Organosilicon Compounds*, Ellis Horwood, Chichester, 1989, p. 235; H. W. Mitzel, J. Riede and H. Schmidbaur, *Acta Crystallogr.*, *Sect. C*, 1996, **52**, 980.
14 S. W. Gurkova, A. I. Gusev, V. A. Sharapov, T. K. Gar and H. V. Alexeev, *J. Struct. Chem.*, 1979, **20**, 302.
15 U. Schubert and C. Steib, *J. Organomet. Chem.*, 1982, **238**, C1; N. Wiberg, C. M. M. Finger, H. Auer and K. Polborn, *J. Organomet. Chem.*, 1996, **521**, 377.
16 C. Eaborn, K. Izod and J. D. Smith, *J. Organomet. Chem.*, 1995, **500**, 89 and references therein; S. S. Al-Juaid, C. Eaborn, A. Habtemariam, P. B. Hitchcock, J. D. Smith, K. Tavakkoli and A. D. Webb, *J. Organomet. Chem.*, 1993, **462**, 45; S. S. Al-Juaid, M. Al-Rawi, C. Eaborn, P. B. Hitchcock and J. D. Smith, 1998, **564**, 215.
17 C. Eaborn, P. B. Hitchcock and P. D. Lickiss, *J. Organomet. Chem.*, 1983, **252**, 281; L. H. Gade, C. Becker and J. W. Lauher, *Inorg. Chem.*, 1993, **32**, 2308.
18 Gaussian 98, Revision A.7, M. J. Frisch, G. W. Trucks, H. B. Schlegel, G. E. Scuseria, M. A. Robb, J. R. Cheeseman, V. G. Zakrzewski, J. A. Montgomery, Jr., R. E. Stratmann, J. C. Burant, S. Dapprich, J. M. Millam, A. D. Daniels, K. N. Kudin, M. C. Strain, O. Farkas, J. Tomasi, V. Barone, M. Cossi, R. Cammi, B. Mennucci, C. Pomelli, C. Adamo, S. Clifford, J. Ochterski, G. A. Petersson, P. Y. Ayala, Q. Cui, K. Morokuma, D. K. Malick, A. D. Rabuck, K. Raghavachari, J. B. Foresman, J. Cioslowski, J. V. Ortiz, A. G. Baboul, B. B. Stefanov, G. Liu, A. Liashenko, P. Piskorz, I. Komaromi, R. Gomperts, R. L. Martin, D. J. Fox, T. Keith, M. A. Al-Laham, C. Y. Peng, A. Nanayakkara, C. Gonzalez, M. Challacombe, P. M. W. Gill, B. Johnson, W. Chen, M. W. Wong, J. L. Andres, C. Gonzalez, M. Head-Gordon, E. S. Replogle and J. A. Pople, Gaussian, Inc., Pittsburgh, PA, 1998.
19 ASYM40 version 3.0, update of program ASYM20. L. Hedberg and I. M. Mills, *J. Mol. Spectrosc.*, 1993, **160**, 117.
20 C. M. Huntley, G. S. Laurenson and D. W. H. Rankin, *J. Chem. Soc.*, *Dalton Trans.*, 1980, 954.
21 J. R. Lewis, P. T. Brain and D. W. H. Rankin, *Spectrum*, 1997, **15**, 7.
22 W. Ross, M. Fink and R. Hilderbrandt, in A. J. C. Wilson (Ed.), *International Tables for Crystallography*, Vol. C, Kluwer Academic Publishers, Dordrecht, 1992, p. 245.
23 S. Cradock, J. Koprowski and D. W. H. Rankin, *J. Mol. Struct.*, 1981, **77**, 113.